Nuclear Physics B283 (1987) 141–164
North-Holland, Amsterdam

STRING MODEL POTENTIALS AND LATTICE GAUGE THEORIES*

M. FLENSBURG† and C. PETERSON

Department of Theoretical Physics, University of Lund, Sölvegatan 14 A, S 22362 Lund, Sweden

Received 2 May 1986

The static potentials from bosonic string models are examined to the two-loop level. Available MC data for 4-dimensional SU(3) are in approximate agreement with the universal leading order predictions but fail to reproduce the Nambu string when the two-loop terms are included in the analysis. We also confront Nambu string model predictions for $T_c/\sqrt{\sigma}$ with SU(2), SU(3) and SU($N \to \infty$) MC data. In the SU(2) case, impressive agreement is found both in 3 and 4 dimensions. In contrast, the data for SU(3) and SU($N \to \infty$) differ from the string model prediction. These theories have identical values for $T_c/\sqrt{\sigma}$, indicating that $N \to \infty$ is a good approximation to $N = 3$.

1. Introduction

It is now generally believed that nonabelian gauge theories have confinement in terms of a linear force law at large distances. This feature is present in strong coupling expansions [1] and more importantly, it has been observed in the approximate continuum limit in lattice Monte Carlo calculations [2]. Still, we lack firm knowledge about the actual confining mechanism. The current picture is that of a thin flux tube (string) joining the quark and antiquark. Models for strings, e.g. the Nambu string [3], have been around since even before the advent of quantum chromodynamics in order to explain phenomenological duality in hadron-hadron interactions and linearly rising Regge trajectories. Although these string models are plagued with ultraviolet problems in 4 space-time dimensions [4], they should make sense as *effective theories at large distances*.

What signature from a string theory would then be visible in lattice Monte Carlo data? The answer is *roughening*. Classically a string is a perfectly stable object, as demonstrated by the existence of the Nielsen-Olesen vortex solution [5]. However, on the quantum mechanical level the string is allowed to vibrate in the transverse directions with long wavelengths $\lambda \sim 1/\text{energy}$ [6]. These roughening fluctuations delocalize the string as the sources are pulled apart. In principle one could verify this feature in lattice Monte Carlo data by measuring the *energy-density distribu-*

* Work supported in part by the Swedish Natural Science Council under contract NFR F 7017-109.
† Present address: NORDITA, Blegdamsvej 17, DK-2100 Copenhagen, Denmark.

0550-3213/87/$03.50

tions. With vacuum configurations at our disposal this is very difficult since it involves normalized correlations between plaquettes and large Wilson loops [7,8]. The ideal pathway would rather be to generate configurations including the source charges and thereby avoid the exponential penalty associated with large Wilson loops. As is well known this requires the development of algorithms dealing with complex actions; a nontrivial problem. For compact $U(1)_3$ this problem was circumvented by using the dual action [9] and convincing direct evidence for the string picture was found [10]. For the nonabelian case the complex Langevin equation has been tried to approach this problem [11].

The roughening fluctuations also give rise to $1/R^n$ *corrections to the linear potential*. The main purpose of this work is to confront these $1/R^n$ corrections with lattice Monte Carlo data for scalar string models. The pioneering work here is due to Lüscher and collaborators [6], who obtained for the leading roughening contribution to the potential

$$V_1(R) = (d-2)\frac{\pi}{24}\frac{1}{R} \tag{1.1}$$

in d space-time dimensions. The result of eq. (1.1) is universal in the sense that it does not depend on the particular string model under consideration for a general class of string theories. This universal Coulomb term is of long-distance character and should of course not be confused with the short-distance, real Coulomb potential

$$V_C(R) = -\tfrac{4}{3}\alpha_s\frac{1}{R}, \tag{1.2}$$

which is dominated by one-gluon exchange.

Eq. (1.1) was derived under very general circumstances. By considering a more restricted class of string models, the Nambu string and variants thereof, Alvarez [12] was able to derive a complete expression for the interquark potential in a $1/d$ expansion

$$V(R) = \sigma R\sqrt{1 - R_c^2/R^2}, \tag{1.3}$$

where R_c is the critical distance

$$R_c = \sqrt{\frac{\pi(d-2)}{12\sigma}} \tag{1.4}$$

beyond which the strong picture breaks down. Eq. (1.3) has subsequently been rederived for any d in the case of the Nambu string [13].

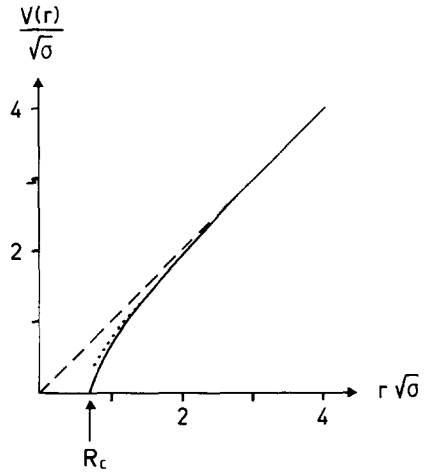

Fig. 1. The Nambu string potential (eq. (1.3)) in 4 dimensions (full line). The dashed and dotted lines denote the second and third terms in the series expansion of eq. (1.5) respectively.

By expanding eq. (1.3) for large distances R one obtains

$$V(R) = V_0(R) + V_1(R) + V_2(R) + \cdots$$

$$= \sigma R - \tfrac{1}{24}\pi(d-2)\frac{1}{R} - \frac{\pi^2}{2\cdot 24^2}(d-2)^2\frac{1}{\sigma R^3} + \cdots, \qquad (1.5)$$

where one, in addition to the linear term, recovers the universal Coulomb term of eq. (1.1). In contrast to the latter the higher order terms will contain powers of a dimensional constant (σ). The potential of eq. (1.5) is shown in fig. 1 as a function of the dimensionless variable $r\sqrt{\sigma}$. The appearance of a critical distance R_c (eq. (1.4)) is not surprising in the light of the problems one encounters in the ultraviolet sector of string theories; these theories should only be used as effective theories at large distances.

When analysing lattice Monte Carlo data with respect to roughening one should use the Wilson or Polyakov loop counterparts of eqs. (1.3) and (1.5) in order to account for the finite T effects properly. These are related to the potential $V(R)$ through

$$V(R) = -\lim_{T\to\infty}\frac{1}{T}\log W(R,T), \qquad (1.6a)$$

$$V(R) = -\lim_{T\to\infty}\frac{1}{T}\log P(R,T), \qquad (1.6b)$$

respectively. In ref. [14] the (universal) first-order predictions $W_1(R,T)$ were

successfully confronted with MC data on SU(2) in 3 dimensions. The situation in this case is somewhat ideal: it is easy to obtain high statistics in 3 dimensions, the short-distance Coulomb term ($\sim \log R$) is easy to distinguish from the roughening piece (eq. (1.1)) and higher order terms are in eq. (1.5) small ($\sim (d-2))^2$. In this work we compare strong model predictions for $W_1(R,T)$ and $W_2(R,T)$ with existing high statistics SU(3) data in 4 dimensions. We have previously reported [15] reasonable agreement for the universal piece $W_1(R,T)$ for $\beta \geq 6.0$. Here we extend this analysis to $\beta < 6.0$ and also compute $W_2(R,T)$ for different scalar string models and compare it with data. (Encouraging results found for the universal piece in terms of Polyakov loops have also been reported for SU(3) [16].) Our result can be summarized as follows. With appropriate cuts on the data ($R > R_c$) we have:

(i) Approximate scaling for σ for $\beta \geq 6.0$.

(ii) For the coefficient in the universal prediction (eq. (1.1)) we obtain 0.30–0.33 as compared the theoretical value 0.26.

(iii) For the (strong model dependent) 2nd order contributions the Nambu string predictions are $\sim$ a factor 8 times larger than what is observed. However, the (R,T) behaviour is consistent with the MC data.

Effective string theories also describe the transition of confined gauge theories into their high temperature plasma phase [17]. By computing the temperature dependence of $V(R)$ the counterparts of eqs. (1.3)–(1.5) are obtained. In particular one gets for the critical temperature T_c (cf. eq. (1.4))

$$T_c = \sqrt{\frac{3\sigma}{\pi(d-2)}} \tag{1.7}$$

for the Nambu string. Hence the value for $T_c/\sqrt{\sigma}$ for *this particular string model* can be compared with MC data on finite T systems. We have performed careful comparisons and find:

(i) $T_c/\sqrt{\sigma}$ from MC results for 3- and 4-dimensional SU(2) agree very well with the predictions of eq. (1.7).

(ii) This is not the case for SU(3) and SU($N \to \infty$) where a significantly lower value is favoured by the MC data.

(iii) $T_c/\sqrt{\sigma}$ for SU(3) equals the corresponding value for SU(64) within the errors. Hence the $N \to \infty$ limit seems to be appropriate for bulk quantities.

This paper is organized as follows. In sect. 2 we briefly review the derivation of the string model results for Wilson and Polyakov loops for the first- and second-order roughening terms. A general discussion on how to extract nonperturbative physics from Monte Carlo data can be found in sect. 3. In sect. 4 we confront the string model predictions for $W_1(R,T)$ and $W_2(R,T)$ with available high statistics SU(3) Monte Carlo data. A crude string model analysis of SU($N \to \infty$) can be found in sect. 5. Predictions for the finite temperature behaviour of string theories are compared with Monte Carlo data in sect. 6 and finally a short summary and discussion can be found in sect. 7.

2. String model potentials

The action for the Nambu string is given by [3]

$$S^{\mathrm{N}} = \sigma \int \left(\frac{1}{2} \frac{\partial(x_\mu, x_\nu)}{\partial(\tau, \rho)} \right)^2 \partial(\tau, \rho), \tag{2.1}$$

which is invariant under reparametrization of τ and ρ. Making the choice $\rho = z$ and $\tau = t$, eq. (2.1) reduces to

$$S^{\mathrm{N}} = \sigma \int\int \mathrm{d}t\, \mathrm{d}z \left(1 + \left(\frac{\partial \bar{x}_\perp}{\partial t} \right)^2 + \left(\frac{\partial \bar{x}_\perp}{\partial z} \right)^2 + \left(\frac{\partial \bar{x}_\perp}{\partial t} \times \frac{\partial \bar{x}_\perp}{\partial z} \right)^2 \right)^{1/2}. \tag{2.2}$$

Eq. (2.2) describes the physics of a string connecting 2 static sources located at $z = 0$ and $Z = R$ evolving in euclidean time from $t = 0$ to $t = T$ with the transverse coordinates $\bar{x}_\perp(t, z)$ subject to appropriate boundary conditions. By expanding the square root in eq. (2.2), S^{N} is factorized into a "classical" minimal sheet times an effective low-energy transverse action.

$$S^{\mathrm{N}} = \mathrm{e}^{-\sigma RT} S^{\mathrm{N}}_{\mathrm{eff}},$$

$$S^{\mathrm{N}}_{\mathrm{eff}} = \tfrac{1}{2}\sigma \int\int \mathrm{d}t\, \mathrm{d}z \left\{ (\nabla \bar{x}_\perp)^2 - \tfrac{1}{4}\left[(\nabla \bar{x}_\perp)^2 \right]^2 + \left(\frac{\partial \bar{x}_\perp}{\partial t} \times \frac{\partial \bar{x}_\perp}{\partial z} \right)^2 \cdots + \right\}. \tag{2.3}$$

Other string models, e.g. the Schild string [18], give rise to similar transverse actions. It was pointed out by Lüscher [6] that for a whole class of string theories subject to general constraints like Poincare and O(2) invariance one has

$$\begin{aligned} S_{\mathrm{eff}} &= \tfrac{1}{2}\sigma \int\int \mathrm{d}t\, \mathrm{d}z \left((\nabla \bar{x}_\perp)^2 + \alpha (\nabla \bar{x}_\perp)^4 + \cdots \right) \\ &= S^{(1)}_{\mathrm{eff}} + S^{(2)}_{\mathrm{eff}} + \cdots, \end{aligned} \tag{2.4}$$

where the first term, $S^{(1)}_{\mathrm{eff}}$, is universal in the sense that it is independent of the details of the string theory under consideration. Thus when comparing with lattice Monte Carlo data the presence of $S^{(1)}_{\mathrm{eff}}$ signals the existence of a scalar string and the higher order terms ($S^{(2)}_{\mathrm{eff}}, \ldots$) should single out a particular string model.

One should observe that actions of the form in eq. (2.4) are not renormalizable by simple power counting arguments. However, it turns out that contributions from $S^{(1)}_{\mathrm{eff}}$ are calculable independent of regularization procedure [6]. Also for $S^{(2)}_{\mathrm{eff}}$ arguments have been presented [19] in favour of renormalizability. Let us first briefly review how to compute the leading universal (one-loop) contributions to

Wilson and Polyakov loops and then proceed to the model dependent and hence more ambiguous second-order (two-loop) terms.

2.1. ONE-LOOP CONTRIBUTIONS

The contribution from $S_{\text{eff}}^{(1)}$ to the partition function over a $R \cdot T$ loop is given by

$$\int \mathrm{D}\bar{x}_1 \exp\left(-\tfrac{1}{2}\sigma \int\int \mathrm{d}t\,\mathrm{d}z\,(\nabla \bar{x}_\perp)^2\right) = \det(-\nabla^2)^{(d-2)/2}, \tag{2.5}$$

where

$$\mathrm{D}\bar{x}_\perp = \prod_i^{d-2} \mathrm{D}x_1^{(i)}.$$

For the *Wilson loop*, where one has Dirichlet boundary conditions

$$\bar{x}_\perp = 0 \qquad \text{on the } R \cdot T \text{ boundary}, \tag{2.6a}$$

the spectrum of the laplacian $-\nabla^2$ is given by

$$\omega_{\mathrm{D}}^2 = \pi^2\left(\frac{m^2}{T^2} + \frac{n^2}{R^2}\right), \qquad m, n = 0, 1, 2, \ldots . \tag{2.6b}$$

In the case of a *Polyakov loop* one instead has periodic boundary conditions in the time direction

$$\begin{aligned} &\bar{x}_\perp(R,0) = \bar{x}_\perp(R,T), \\ &\bar{x}_\perp(0,T) = \bar{x}_\perp(R,T) = 0, \end{aligned} \tag{2.7a}$$

which yields the spectrum

$$\omega_{\mathrm{P}}^2 = \pi^2\left(4\frac{m^2}{T^2} + \frac{n^2}{R^2}\right), \qquad \begin{matrix} m = 0, \pm 1, \pm 2, \ldots \\ n = 0, 1, 2, \ldots \end{matrix} . \tag{2.7b}$$

The calculation of the determinant of eq. (2.5) thus involves infinite mode sums. These are conveniently handled with ζ-function regularization. One finds [14, 19]

$$\det(-\nabla_{\mathrm{D}}^2) = \frac{1}{\sqrt{2R}}\eta\left(i\frac{T}{R}\right), \tag{2.7c}$$

$$\det(-\nabla_{\mathrm{P}}^2) = \eta^2\left(i\frac{T}{2R}\right), \tag{2.7d}$$

where we have used the Dedekind η-function

$$\eta(\phi) = e^{i\pi\phi/12} \prod_{n=1}^{\infty} (1 - e^{2\pi i\phi n}). \tag{2.8}$$

The contribution from $S_{\text{eff}}^{(1)}$ to the Wilson loop is then given by

$$-\log W_1(R,T) = (d-2)\left[-\frac{\pi}{24}\frac{T}{R} - \tfrac{1}{4}\log R + \tfrac{1}{2}\sum_{n=1}^{\infty}\log(1 - e^{-2\pi nT/R})\right]. \tag{2.9}$$

As can be seen from the η-function inversion formula,

$$\eta(\phi) = \left(\frac{i}{\phi}\right)^{1/2} \eta\left(-\frac{1}{\phi}\right), \tag{2.10}$$

eq. (2.9) is symmetric in R and T despite its asymmetric appearance. For the Polyakov loop one instead obtains

$$-\log P_1(R,T) = (d-2)\left[-\frac{\pi}{24}\frac{T}{R} + \sum_{n=1}^{\infty}\log(1 - e^{-\pi nT/R})\right]. \tag{2.11}$$

Using the definition in eq. (1.6) one obtains from eqs. (2.9) and (2.1) in the $T \to \infty$ limit eq. (1.1). The resulting $1/R$ term in eq. (1.1) is universal and of long-distance origin. It depends on no other parameters than the number of transverse dimensions, $(d-2)$, in which the string lives.

Polyakov loops are usually measured with $T < R$ rather than $T \gg R$. In this limit the second term in eq. (2.11) dominates. By utilizing the $R \leftrightarrow T$ symmetry of eq. (2.9) for $W(2R,T)$ this term can be rewritten as

$$\sum_{n=1}^{\infty}\log(1 - e^{-\pi nT/R}) = \frac{\pi}{24}\frac{T}{R} - \frac{\pi}{6}\frac{R}{T} + \sum_{n=1}^{\infty}\log(1 - e^{-4\pi nT/R}), \tag{2.12}$$

and one gets [20]

$$-\log P_1(R,T) = (d-2)\left[-\frac{\pi}{6}\frac{R}{T} - \tfrac{1}{2}\log\frac{T}{2R} + \sum_{n=1}^{\infty}\log(1 - e^{-4\pi nR/T})\right]. \tag{2.13}$$

The R/T term in eq. (2.13) represents a "universal finite temperature" correction for $R < T$ and is in fact larger in magnitude than the T/R term in eq. (2.9). Hence Polyakov loops are very sensitive to roughening contributions.

2.2. TWO-LOOP CONTRIBUTIONS

As already stated above only the leading (one-loop) vibrational energies are universal in the sense that they do not depend on the details of the string theory. However with the advent of very accurate data on relatively large Wilson loops it might be interesting to confront particular string models (e.g. the Nambu string) with Monte Carlo data. This requires the calculation of terms in the potential originating from the higher order terms in eqs. (2.3) and (2.4). This was done to the two-loop level in ref. [19]. We will below quote and discuss these results.

Expectation values $\langle A \rangle$ from the higher order terms in eq. (2.3) are defined by

$$\langle A \rangle = \frac{\int \mathrm{D}\bar{x}_1 \, A \exp\left(-\frac{1}{2}\sigma \int\int st \, \mathrm{d}z \left(\nabla \bar{x}_\perp\right)^2\right)}{\int \mathrm{D}\bar{x}_1 \exp\left(-\frac{1}{2}\sigma \int\int \mathrm{d}t \, \mathrm{d}z \left(\nabla \bar{x}_\perp\right)^2\right)} . \tag{2.14}$$

Using the eigenfunctions corresponding to the eigenvalues of eq. (2.6) for computing the higher order terms one encounters a sum of divergent expressions, which again can be regularized by ξ-function techniques. A typical term in the sum has the form

$$\sum_{m,n=1}^{\infty} \frac{m^2}{m^2/T^2 + n^2/R^2} = \tfrac{1}{2}\pi RT\xi(-1) + \tfrac{1}{2}T^2\xi(0) + \pi RT \sum_{m=1}^{\infty} \frac{m}{\mathrm{e}^{2m\pi R/T} - 1}$$

$$= \frac{\pi}{24}\frac{T^3}{R}\left(-i\frac{12}{\pi}\right)\left[\partial_\tau \log \eta(\tau)\right]_{\tau = iT/R} . \tag{2.15}$$

In ref. [19] the contribution from these kind of terms were computed for a class of scalar string actions defined by

$$S_{\mathrm{eff}} = \tfrac{1}{2}\sigma \int\int_{R\cdot T} \mathrm{d}t \, \mathrm{d}z \left\{ \left(\nabla \bar{x}_\perp\right)^2 + \lambda_1 \left(\frac{\partial \bar{x}_\perp}{\partial t} \times \frac{\partial \bar{x}_\perp}{\partial z} \right)^2 + \lambda_2 \left[\left(\nabla \bar{x}_1\right)^2 \right]^2 \right\} . \tag{2.16}$$

The Nambu string of eq. (2.3) is recovered with $\lambda_1 = 1$ and $\lambda_2 = -\frac{1}{4}$. We now list the results for the two-loop contributions from the effective action of eq. (2.16).

(1) Dirichlet boundary conditions (Wilson loops). One gets [19]

$$-\log W_2(R,T)$$

$$= \frac{T}{\sigma R^3}\tfrac{1}{4}\Big\{ \left[(d-2)^2\left(\tfrac{1}{2}\lambda_1\right) + (d-2)\left(2\lambda_2 + \tfrac{1}{2}\lambda_1\right) \right] \left(\partial_\tau \log \eta(\tau)\right)^2$$

$$- \tfrac{1}{2}\left[(d-2)^2(\lambda_1 + 4\lambda_2) + (d-2)(4\lambda_2 - \lambda_1) \right] \partial_\tau^2 \log \eta(\tau)$$

$$- \tfrac{1}{2}\Big[(d-2)^2\left(\tfrac{3}{2}\lambda_1 + 4\lambda_2\right)$$

$$+ (d-2)\left(2\lambda_2 - \tfrac{3}{2}\lambda_1\right) \Big] \frac{1}{\tau}\, \partial_\tau \log \eta(\tau) \Big\}_{\tau = iT/R} . \tag{2.17}$$

For the Nambu string one then has

$$-\log W_2(R,T)$$
$$= \frac{T}{4\sigma R^3}\Big\{(d-2)\,\partial_\tau^2 \log\eta(\tau) - \tfrac{1}{2}(d-2)^2\big(\partial_\tau \log\eta(\tau)\big)^2$$
$$+\Big[-\tfrac{1}{4}(d-2)^2 + (d-2)\Big]\frac{1}{\tau}\,\partial_\tau \log\eta(\tau)\Big\}_{\tau=iT/R}. \quad (2.18)$$

For the (R,T) region of interest, eq. (2.18) can be conveniently parametrized as

$$-\log W_2(R,T) \approx -0.0662\frac{1}{\sigma}\left(\frac{T}{R^3}+\frac{R}{T^3}\right). \quad (2.19)$$

Using the $\tau \to \infty$ limits $\partial_\tau \log\eta(\tau) \to -\frac{1}{12}\pi$, $\partial_\tau^2 \log\eta(\tau) \to 0$ and $\partial_\tau \log\eta(\tau)/\tau \to 0$ the corresponding potential in $(d-2)$ transverse dimensions (eq. (1.6a)) reads

$$V(R) = -\tfrac{1}{2}(d-2)^2\left(\frac{\pi}{24}\right)^2\frac{1}{\sigma R^3}. \quad (2.20)$$

We observe that this $1/R^3$ contribution corresponds to the third term in the expansion of the Alvarez-Arvis potential in eq. (1.5). This is not necessarily true for all scalar string models of the form in eq. (2.16). For example the Schild model [18] gives a two-loop contribution different from eq. (2.19) [19].

(2) Time periodic boundary conditions (Polyakov loops). For completeness we also give the corresponding two-loop contribution in this case. For the Polyakov loop it reads

$$-\log P_2(R,T)$$
$$-\frac{T}{\sigma R^3}\tfrac{1}{8}\Big\{\big[(d-2)(d-3)\lambda_1 - 4(d-2)\lambda_2\big]\big(\partial_\tau \log\eta(\tau)\big)^2$$
$$+\big[(d-2)(d-3)\lambda_1 + 4(d-1)(d-2)\lambda_2\big]\,\partial_\tau^2 \log\eta(\tau)\Big\}_{\tau=iT/R}. \quad (2.21)$$

For the Nambu string, eq. (2.20) reduces to

$$-\log P_2(R,T) = -\frac{T}{\sigma R^3}\tfrac{1}{8}\Big[(d-2)^2\big(\partial_\tau \log\eta(\tau)\big)^2 - (d-2)\,\partial_\tau^2 \log\eta(\tau)\Big]_{\tau=iT/R}, \quad (2.22)$$

from which one in the $\tau \to \infty$ limit recovers eq. (2.18). It is satisfying (although not a proof) from the point of view of regularization procedure consistence that one obtains identical results with the different boundary conditions.

3. Extracting non-perturbative physics from lattice Monte Carlo data

The interquark potential can be extracted either from Wilson or Polyakov loops (eq. (1.6)). Each method has its disadvantage: Wilson loops are exponentially suppressed at large R whereas Polyakov loops at large distances often have $T < R$ and hence contain substantial finite T effects. (This latter feature turns out to be advantageous, however, for obtaining a strong roughening signal as discussed above.) In the approximate scaling region, $\beta \geqslant 6.0$, most available high statistics data are for Wilson loops. We therefore focus on these.

Which Wilson loop sizes are relevant for comparison with nonperturbative string physics? A guideline is given by the Alvarez bound (eq. (1.4)). For 3- and 4-dimensional theories one has $R_c^{np} \approx 0.5/\sqrt{\sigma(\beta)}$ and $0.7/\sqrt{\sigma(\beta)}$ respectively. In fig. 2 the physical distances for SU(3) are shown as functions of β for different values of R in $W(R, T \geqslant R)$. The physical distance scale has been normalized according to the asymptotic freedom prediction

$$a(\beta) = \frac{1}{\Lambda_L}\left(\tfrac{8}{33}\pi^2\beta\right)^{51/121}\exp\left(-\tfrac{4}{33}\pi^2\beta\right), \tag{3.1}$$

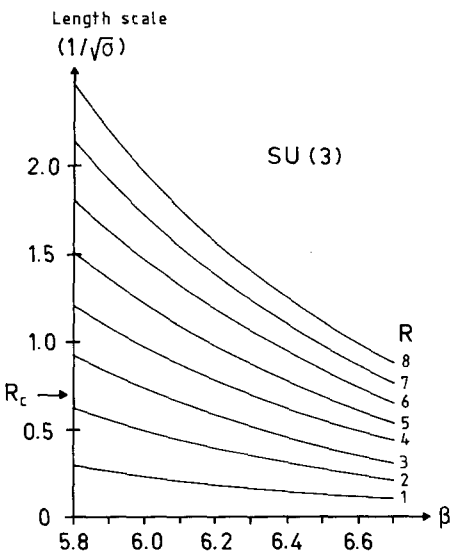

Fig. 2. Physical distances as functions of β for different R. Normalized according to eq. (4.3).

with $\Lambda_L/\sqrt{\sigma} \approx 0.01$ [21,22,15]. Since the maximal values of R for measured $W(R,T)$ are rather small (see table 1) R_c^{np} puts severe constraints on the data analysis. There is another thing one should keep in mind. Despite recent attempts to reduce the variance large loops have much larger relative errors than the smaller ones. Hence when fitting theoretical expressions like eq. (2.9) to MC data one inevitably weights smaller distances more heavily than the larger ones. This contrasts our aim to investigate large distance physics.

Since the perturbative short distance Coulomb potential (eq. (1.2)) has the same R-behaviour as the leading roughing term (eq. (1.1)) in 4 dimensions one should examine the behaviour of the lattice Coulomb potential [23].

$$V(R) = \tfrac{16}{33}\pi \frac{1}{R \log\left(1/(\Lambda_p R)^2\right)} \left(1 - \frac{102}{121} \frac{\log\log\left(1(\Lambda_p R)^2\right)}{\log\left(1/(\Lambda_p R)^2\right)}\right). \tag{3.2}$$

Eq. (3.2), which is shown in fig. 3, exhibits for $\Lambda_L/\sqrt{\sigma} = 0.01$ [21,22,15] and $\Lambda_p = 82.07\,\Lambda_L$ a maximum around $R_m^{pert} \approx 0.4/\sqrt{\sigma(\beta)}$. Beyond that value $V(R)$ drops as the perturbation theory breaks down.

TABLE 1
Parameter values θ_i as obtained by fitting eq. (4.2) to the different data sets

β	θ_1	θ_2	θ_3	θ_4	R_{min}	max $R \cdot T$	Lattice size	Ref.
5.8	0.0970	0.687	−0.343	−0.540	3	6·8	16^4	22
5.8	0.1114	0.619	−0.368	−0.307	3	5·7	16^4	24
6.0	0.0510	0.653	−0.386	−0.500	3	8·8	16^4	25
6.0	0.0518	0.639	−0.328	−0.413	3	8·8	16^4	26
6.0	0.0581	0.615	−0.316	−0.429	3	6·8	16^4	22
6.1	0.0351	0.647	−0.383	−0.503	3	8·12	20^4	27
6.2	0.0350	0.605	−0.345	−0.428	3	6·8	16^4	22
6.3	0.0232	0.600	−0.313	−0.396	3	8·8	16^4	26
6.3	0.0247	0.597	−0.301	−0.403	3	12·12	24^4	28
	0.0226	0.604	−0.306	−0.420	4			
	0.0211	0.616	−0.350	−0.496	5			
6.3	0.0224	0.610	−0.321	−0.468	3	8·12	20^4	27
	0.0234	0.608	−0.327	−0.529	4			
6.4	0.0205	0.587	−0.339	−0.424	3	6·8	16^4	22
average values:			−0.334	−0.438				
theoretical predictions:			−0.26	−0.5				

R_{min} is the minimal R used in the fits. The maximal $R \cdot T$ used in our fits are also given. The average values for θ_3 and θ_4 are calculated for $\beta \geq 6.0$ and $R_{min} = 3$.

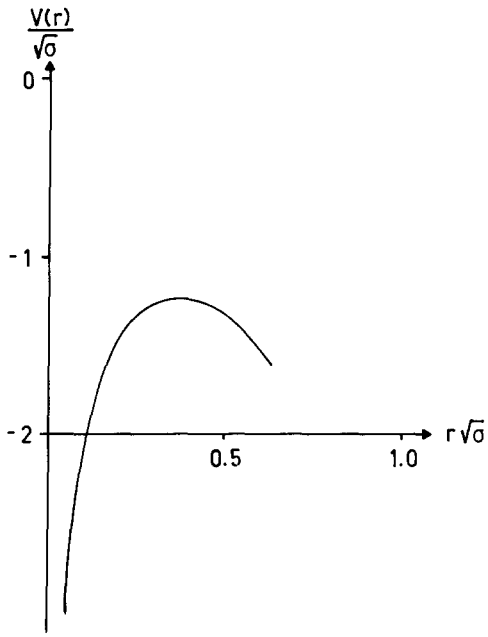

Fig. 3. The perturbative Coulomb potential of eq. (3.2) with $\Lambda_L/\sqrt{\sigma} = 0.01$.

4. Analysis of the SU(3) lattice potential

Let us first confront the SU(3) lattice Monte Carlo data with the leading universal string model prediction of eq. (2.9) and then proceed with the two-loop contribution, eq. (2.18).

4.1. THE LEADING STRING MODEL CONTRIBUTION

We start by subtracting from the measured values of $-\log W(R,T)$ the last term of eq. (2.9),

$$(d-2)\tfrac{1}{2}\sum_{1}^{\infty}\log(1-\mathrm{e}^{-2\pi nT/R}), \tag{4.1}$$

which amounts to a very small correction unless $T < R - 1$. Guided by eq. (2.9) and allowing for an area, a perimeter and a constant term we fit to the expression

$$\begin{aligned} &-\log W(R,T) - (d-2)\tfrac{1}{2}\sum_{1}^{\infty}\log(1-\mathrm{e}^{-2\pi nT/R}) \\ &\quad = \theta_1 RT + \theta_2(R+T) + \theta_3 T/R + \theta_4 \log R + \theta_5 \\ &\quad = (\theta_1 R + \theta_2 + \theta_3/R)T + [\theta_2 R + \theta_4 \log R + \theta_5], \end{aligned} \tag{4.2}$$

which is linear in T. For each pair of R and β with $R \geqslant R_c^{np}$ we fit to a straight line in T. As a result we obtain both slope and intercept for each R and β. We used $R_c^{np} = 3$ for all β-values except for $\beta = 6.3$, where also $R_c^{np} = 4,5$ was used. With some 40 pairs of R and β at our disposal we then perform 2 parameters fits, each to several different values of T. The statistical weights are $W(R,T)/\sigma(R,T)$, where $\sigma(R,T)$ denotes respective standard deviation. Typical χ^2/DOF values lie in the 1–4 range for these fits. The resulting parameters are shown in table 1 and figs. 4 and 5. As can be seen from fig. 4a approximate scaling holds for $\beta \geqslant 6.0$ with

$$\sqrt{\sigma}/\Lambda_L = 0.296 \times 10^2. \tag{4.3}$$

For the coefficient in front of the $1/R$ term we have the average $\langle\theta_3\rangle = -0.334$ which is slightly lower than the theoretical value $-\frac{2}{24}\pi = -0.26$. There is no sign of a roughening transition, $\theta_3 = 0$, for $\beta < 5.8$. For the $\log R$ coefficient we have $\langle\theta_4\rangle = -0.438$ which is slightly below the string model value $2 \cdot \frac{1}{4} = 0.5$. One should keep in mind though that these roughening terms together with the area piece are subdominant contributions as compared to the perimeter term. This fact is illustrated in fig. 6, from which it is also clear that it might be difficult to disentangle the $1/R$ from the $\log R$ piece at moderate R.

What about Polyakov loops (or Wilson lines), where the finite T effects for the strong terms were quite substantial (cf. eq. (2.13))? This question was analysed in ref. [16] with encouraging results.

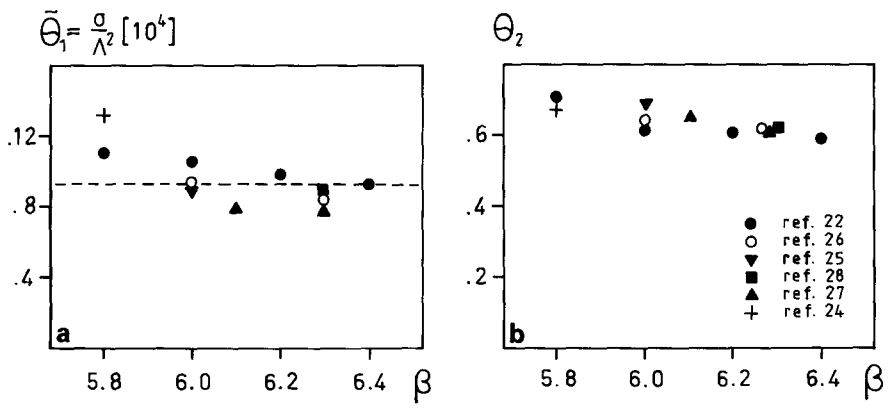

Fig. 4. The parameters θ_1 and θ_2 as defined in eq. (4.2). Instead of θ_1 we have plotted the variable

$$\tilde{\theta}_1 = \frac{\sigma}{\Lambda_L^2} = \theta_1 \left[\tfrac{8}{33}\pi^2\beta\right]^{-102/121} \exp\left(\tfrac{8}{33}\pi^2\beta\right).$$

The dashed line corresponds to eq. (4.3).

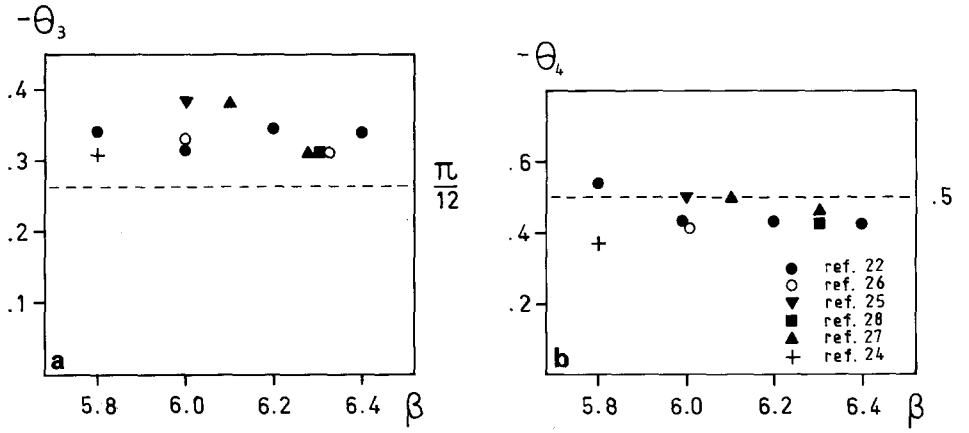

Fig. 5. The parameters θ_3 and θ_4 as defined in eq. (4.2). The dashed lines are the (leading order) string model predictions of eq. (2.9).

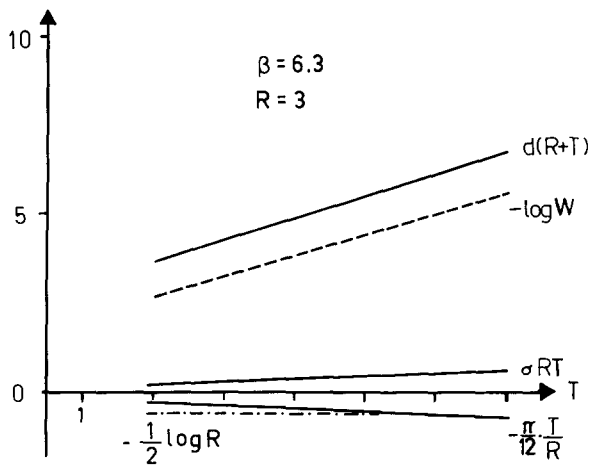

Fig. 6. A typical decomposition of $-\log W(R,T)$ into perimeter, area, and the vibrational terms of eq. (2.9). Data from ref. [28].

4.2. TWO-LOOP CONTRIBUTIONS

In order to pin down the Nambu string we have included the second-order contribution (eq. (2.18) into eq. (4.2)) and fitted the data of ref. [27] with one additional parameter. We find that the resulting old parameters θ_1, θ_2, θ_3 and θ_4 are essentially unchanged. The coefficient in front of the second-order term in eqs. (2.18) and (2.19) is a factor ~ 8 smaller than predicted. However, the inclusion of this term takes care of the nonlinearity in T previously reported [15]. This deviation from linearity is shown in fig. 7a, where the difference between $-\log W(R,T)_{\text{data}}$

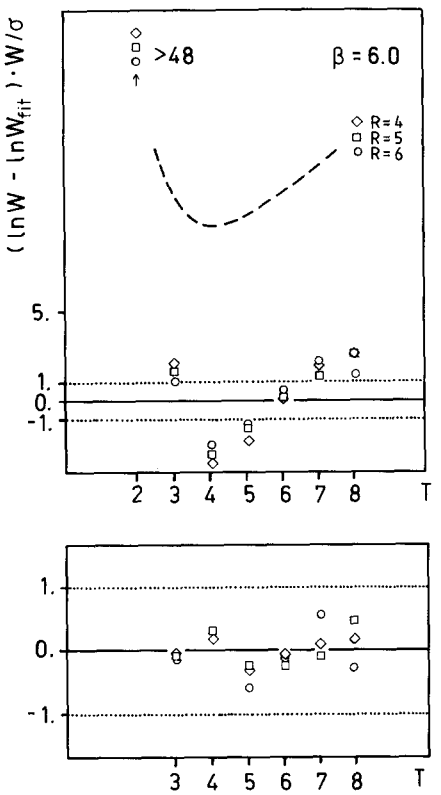

Fig. 7. (a) Deviation of eq. (4.2) from a straight line in T for $R = 4$, 5 and 6 at $\beta = 6.0$ [22]. The dashed line shows the functional form of the higher order correction (eqs. (2.18) and (2.19)). (b) The same deviation as in (a) after including eq. (2.18) in the fit. The resulting coefficient of eq. (2.19) is $= -0.008$.

and $-\log W(R,T)_{\text{fit}}$ is plotted from lowest order fits. One notes a small but systematic deviation (the same pattern occurs for other β and R values). Also shown in fig. 7a is the functional form of the second order term of eq. (2.18). In fig. 7b the same quantity is shown with the second-order Nambu term included in the analysis. Its fitted magnitude is a factor ~ 8 too small as compared with the prediction. It is clear from fig. 7 that the functional form of eq. (2.18) is consistent with the MC data though.

In order to further study the effects from higher order contributions we project out the vibrational part of $-W(R,T)$ by taking the second derivative with respect to R. Including only the lowest order part of the vibrational terms one then has

$$\frac{R^3}{2T}\frac{\partial^2}{\partial R^2}\log W(R,T) = (d-2)\left[\tfrac{1}{24}\pi - \frac{1}{8}\frac{R}{T} - \frac{R^3}{2T}\frac{\partial}{\partial R^2}\tfrac{1}{2}\sum_1^\infty \log(1-\mathrm{e}^{-2\pi nT/R})\right]. \tag{4.4}$$

By constructing the lattice second derivative Δ of $\log W(R,T)$

$$\Delta \log W(R,T) = \log W(R,T) + \log W(R-2,T) - 2\log W(R-1,T), \quad (4.5)$$

one obtains the discretized version of eq. (4.4)

$$\frac{1}{2T}R(R-1)(R-2)\Delta \log W(R,T)$$

$$= (d-2)\left\{\tfrac{1}{24}\pi + \frac{R(R-1)(R-2)}{8T}\log\frac{R(R-2)}{(R-1)^2}\right.$$

$$\left. - \frac{R(R-1)(R-2)}{4T}\Delta\sum_{1}^{\infty}\log(1-e^{-2\pi nT/R})\right\}, \quad (4.6)$$

where only the $n=1$ part of the last term is kept.

Eq. (4.5) agrees very well with data from 3-dimensional SU(2) [14]. We note that even though this quantity is very sensitive to higher order terms, the second

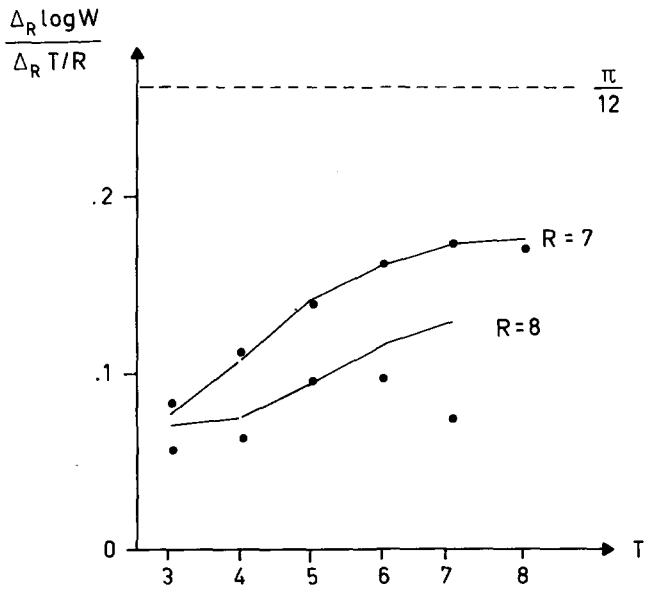

Fig. 8. The discretized second derivative (negative increment) of $\log W$ normalized to make the T/R term constant (eq. (4.6). Thus infinite T loops should give $\frac{1}{12}\pi$ in the string model, whereas no roughening corresponds to zero. The lines represent fits to the data including the second order Nambu contribution, which is small only for $R > 7$. One obtains $\theta_3 = -0.22$ and $\theta_4 = -0.40$ and a Nambu second order coefficient a factor ~ 4 smaller than predicted. All data for $R \geqslant 5$ cannot be fitted well by a string form simultaneously. The errors are not quoted. With standard methods these are too large since Wilson loops with nearby R are strongly correlated.

derivative makes the plausible convergence of the expansion in terms of T/R^n become more critical. Higher order contributions will blow up and the second- and first-order ratio attains a factor of 6 thereby raising the appropriate lower bound from $R_{\min} = 3$ to $R = \sqrt{6}\, R_{\min}$. Thus we are left with the highest R data with poor statistics. As above we find the lower order parameters rather stable. The second-order coefficient comes out a factor ~ 4 too small. We have to conclude though that the second derivative with present data cannot be used to give a definite answer concerning the second-order term in the string potential. In fig. 8 we note however that the lowest order terms give a fairly good description for this quantity.

In summary we conclude that the second order term is there with a shape consistent with the Nambu model but with the wrong absolute magnitude. Similar results hold for the Schild string.

5. The SU($N \to \infty$) lattice potential

It is clear that analysing MC data by means of eq. (4.2) requires a large number of different sized high statistics Wilson loop measurements at our disposal. However, the effects from string roughening also modify the Creutz ratios

$$\chi(R,T) = -\log \frac{W(R,T)\cdot W(R-1,T-1)}{W(R,T-1)\cdot W(R-1,T)}, \tag{5.1}$$

which at large R and T equals σa^2. With the string vibrational terms of eq. (4.2) one obtains modified ratios $\tilde{\chi}(R,T)$ (perimeter and constant terms vanish)

$$\tilde{\chi}(R,T) = \chi(R,T) - (d-2)\frac{\pi}{24}\frac{1}{R(R-1)} + \Delta(R,T), \tag{5.2}$$

where $\Delta(R,T)$ is negligible correction. If strings are there one expects $\tilde{\chi}(R,T)$ to be more constant with R and T than $\chi(R,T)$. Also, the asymptotic freedom scaling of σa^2 should improve when considering $\tilde{\chi}(R,T)$.

For the purpose of $T_c/\sqrt{\sigma}$ considerations to come (see sect. 6) we have investigated *MC data on SU($N \to \infty$)* with respect to this issue. By using the twisted Eguchi-Kawai model, Monte Carlo simulations have been performed for $N = 36$ [29] and $N = 64$ [30]. In fig. 9 we show the results for SU(64) on $\chi(3,3)$ and $\tilde{\chi}(3,3)$ together with the asymptotic freedom curves. It is clear from this figure that the string corrected $\tilde{\chi}(3,3)$ exhibits better scaling than $\chi(R,T)$ with a significantly modified $\sqrt{\sigma}/\Lambda_L$ as a result. One gets

$$\sqrt{\sigma}/\Lambda_L = 213. \tag{5.3}$$

Similar features hold for the SU(36) data.

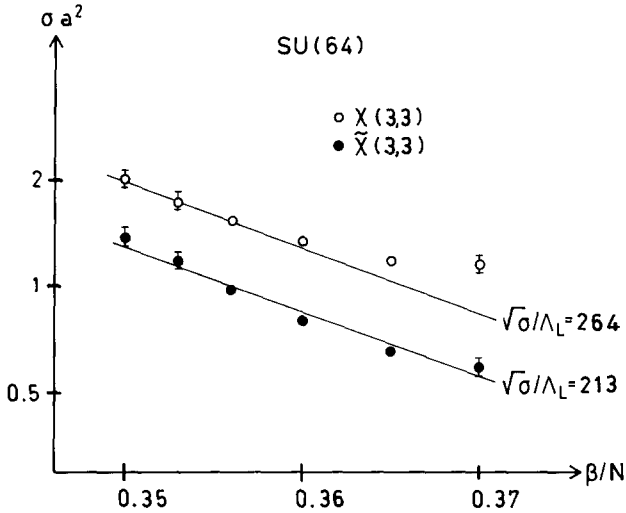

Fig. 9. $\chi(3,3)$ and $\tilde{\chi}(3,3)$ for SU(64). The solid lines give the asymptotic scaling behaviour according to

$$\sigma a^2 = \frac{\sigma}{\Lambda_L^2}\left[\tfrac{8}{11}\pi^2(\beta/N)\right]^{-102/121}\exp\left[\tfrac{8}{11}\pi^2(\beta/N)\right].$$

6. Strings at finite temperature

The lattice MC approach have been very successful in the finite temperature sector. One has good evidence for a deconfining phase transition both for SU(2) [31–34] and SU(3) [36–37] in the quenched approximation and preliminary results now exist when dynamical fermions are included [38]. As clean signatures of this transition one observes sharp rises both in the free energy and in the order parameter given by the Wilson line. Within the framework of the twisted Eguchi-Kawai model, Monte Carlo calculations have also provided good evidence for this transition in the $N \to \infty$ limit [39,40]. The nature of the transition is first order for SU(3), SU(64) and SU(81), whereas for SU(2) the data favours a second order transition.

This deconfining transition appears naturally in string theories [17,41,42] with the following intuitive picture. At $T = 0$ the coloured sources are connected with flux tubes (strings) via the shortest path. Inside the flux tube asymptotic freedom suppresses the interactions and one has the perturbative vacuum in contrast to the surrounding nonperturbative confining vacuum. As the external temperature T increases the string starts to vibrate and the two sources are no longer connected by the shortest path (see fig. 10). The perturbative vacuum is being spread out at the expense of the confining medium. Eventually the perturbative vacuum will take over, confinement is lost and the plasma phase of the theory is reached.

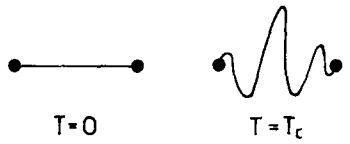

Fig. 10. A string at $T = 0$ and $T = T_c$.

This phenomena can be understood quantitatively by considering the effective string action of eq. (2.3) at finite temperature [17]. At large temperatures confinement is measured by a $R \cdot \beta$ Wilson-loop, where $R > \beta = T^{-1}$. Defining a temperature dependent string tension $\sigma(T)$ through

$$-\log W(R,\beta) = \sigma(T) R \cdot \beta, \tag{6.1}$$

and replacing T by $\beta = T^{-1}$ in eq. (2.13) one obtains for $\sigma(T)$ [17]

$$\sigma(T) = \sigma - (d-2)\left[\tfrac{1}{6}\pi T^2 - \tfrac{1}{2}\log 2RT + \frac{T}{R}\sum_{n=1}^{\infty}\log(1-\mathrm{e}^{-2\pi nRT})\right], \tag{6.2}$$

where $\sigma = \sigma(0)$. The second term in this equation is analogous to the $1/R$ correction of eq. (1.1). It is the leading order term in a series which again can be summed up in a large d expansion at least for the Nambu-Goto string. One obtains [17] (cf. eq. (1.3))

$$\sigma(T) \underset{d\to\infty}{=} \sigma\sqrt{1-(T/T_c)^2}, \tag{6.3}$$

where

$$T_c = \sqrt{\frac{3\sigma}{\pi(d-2)}}. \tag{6.4}$$

So once $\sigma = \sigma(T=0)$ is known the string theory predicts the location of T_c for a given dimensionality.

If one wants to confront the string model predictions (eqs. (6.2)–(6.4)) with MC data one has to keep in mind that the prediction of eq. (6.2) is universal for a class of scalar string theories whereas eqs. (6.3) and (6.4) are model dependent and have only been derived for the Nambu string. On the other hand it is easier to numerically determine T_c (eq. (6.4)) than the detailed T-behaviour of $\sigma(T)$ (eq. (6.2)). No high accuracy MC data is available for $\sigma(T)$ and we will henceforth focus on T_c.

When comparing the string model prediction of eq. (6.2) with MC data one needs the dimensionless ratio $T_c/\sqrt{\sigma}$. The main uncertainty entering this quantity originates

from σ and not T_c itself. As is clear from the previous sections the determination of σ is difficult. Not only is it extracted from an exponentially damped quantity but its determination is (string) model dependent. In table 2 we have compiled available data on T_c and σ and computed $T_c/\sqrt{\sigma}$ for 3-dimensional SU(2) [$SU(2)_3$], SU(2), SU(3) and SU($N = 64$ and 81). The compilation and analysis is restricted to measurements of T_c and σ in the approximative scaling regions. All σ-values quoted have been subject to $1/R$ subtractions. When comparing the theoretical predictions (eq. (6.4))

$$\frac{T_c}{\sqrt{\sigma}} = \sqrt{\frac{3}{\pi(d-2)}} = \begin{cases} 0.97 & \text{(3 dimensions)} \\ 0.69 & \text{(4 dimensions)} \end{cases}, \tag{6.5}$$

very good agreement is found for SU(2) in 3 and 4 dimensions in contrast to SU(3) and SU($N \to \infty$) where the MC data favours a lower value (see table 3).

TABLE 2a

T_c and $\sqrt{\sigma}$ for 3-dimensional SU(2) [$SU(2)_3$] in the quenched approximation

$T_c \cdot \beta a$	$\sqrt{\sigma} \cdot \beta a$	$\langle T_c/\sqrt{\sigma} \rangle$	Nature of transition	Ref.
1.39 ± 0.1				43
			2nd order	
	1.48			14
		$\overline{0.94 \pm 0.03}$		

This theory is super-renormalizable. Hence T_c and σ scale like $1/\beta a$ and $1/(\beta a)^2$, respectively.

TABLE 2b

T_c and $\sqrt{\sigma}$ for SU(2) in the quenched approximation

T_c/Λ_L	$\sqrt{\sigma}/\Lambda$	$\langle T_c/\sqrt{\sigma} \rangle$	Nature transition	Ref.
43*				32
42*			2nd order	33
41				34
	67			44
	53			45
	56			46
	50			47
		$\overline{0.74 \pm 0.10}$		

*Averaged over different N_t.

TABLE 2c
T_c and $\sqrt{\sigma}$ for SU(3) in the quenched approximation

T_c/Λ_L	$\sqrt{\sigma}/\Lambda_L$	$\langle T_c/\sqrt{\sigma}\rangle$	Nature of transition	Ref.
51 ± 2			1st order	36
46.6 ± 0.7				37
	106			21
	104			22
	96			15
		$\overline{0.48 \pm 0.05}$		

TABLE 2d
T_c and $\sqrt{\sigma}$ for SU(N) at large N in the quenched approximation

N	T_c/Λ_L	$\sqrt{\sigma}/\Lambda_L$	$\langle T_c/\sqrt{\sigma}\rangle$	Nature of transition	Ref.
60	$\underline{101 \pm 4}$			1st order	39
64	$\underline{118 \pm 6}$				40
81	107 ± 8*				40
36		241			29 [eq (4.8)]
36		241			30 [eq (4.8)]
64		$\underline{225}$			30 [eq (4.8)]
			$\overline{0.49 \pm 0.04}$		

*Averaged over different N_t.
Only underlined values included in $\langle T_c/\sqrt{\sigma}\rangle$.

TABLE 3
$T_c/\sqrt{\sigma}$ from string theory and MC calculations

Theory	MC results	String model eq. (3.6)
$SU(2)_3$	0.94 ± 0.03	0.97
SU(2)	0.74 ± 0.10	0.69
SU(3)	0.48 ± 0.05	0.69
SU(64)	0.49 ± 0.04	0.69

Another consequence of the Nambu string theory prediction of eq. (6.4) concerns the order of the phase transition. A second-order phase transition is characterized by a correlation length ξ that diverges at $T = T_c$. The correlation length is related to the string tension by

$$\xi(T) = \frac{1}{\sqrt{\sigma(T)}} . \tag{6.6}$$

From eqs. (6.3) and (6.4) it is thus clear that $\xi \to \infty$ as $T \to T_c$. This result is not sensitive to the particular form of eq. (6.3) but is a simple consequence of $\sigma(T \to T_c) \to 0$ in polynomial way. This result can however only be demonstrated for the Nambu string where all orders in the T/T_c expansion have been summed up. Other string models might as well give rise to other kind of transitions. It is in this context interesting to note that for 3- and 4-dimensional SU(2) one indeed observes second-order phase transitions whereas for SU(3) and SU($N \to \infty$) the transitions are of second order. Thus the successful comparisons with the Nambu string model results for $T_c/\sqrt{\sigma}$ coincides with second-order phase transitions. This is another indication that this model is not adequate for SU(3) as observed above in connection with the second-order string vibrational static energies.

We should also mention that there exist alternative string model descriptions of the breakdown of confinement [48], where an effective partition function is constructed out of closed loops for the vacuum. These closed loops represent small fluxes (a gas of glueball, strings) that diverge in configuration space in the vicinity of T_c. For SU(2) one also here has a second order phase transition whereas for SU(3) a first-order transition is plausible if one allows for the strings to interact through baryonic vertices.

We close this section by noting how close the SU(3) and SU($N \to \infty$) values are. The $N \to \infty$ limit really seems to be appropriate for bulk quantities like T_c and σ.

7. Summary

Results. We have compared string model predictions with lattice Monte Carlo data on the static force in SU(3) and the deconfinement temperature in SU(2) and SU(3). This comparison has been pursued on two levels:

(i) The *leading order predictions*, which are universal and independent on the particular choice of string model, are found to be in approximate agreement with SU(3). Appropriate cuts have been made to ensure that the perturbative physics is excluded from the analysis.

(ii) In contrast the *higher order predictions* are model dependent. In the case of the SU(3) static potential second order terms are found to be consistent with MC data with respect to shape but not in magnitude for the Nambu string. Hence this particular string model is not supported by the MC static potential. This feature is

consistent with the situation for $T_c/\sqrt{\sigma}$. The string prediction here is again model dependent. For SU(3) (and SU($N \to \infty$)) a substantial discrepancy is found when confronting the Nambu string with MC data for the critical temperature. This is in contrast to SU(2) in 3 and 4 dimensions where $T_c/\sqrt{\sigma}$ is accurately predicted by the Nambu string model.

Conclusions. For SU(3) an effective scalar string theory seems to be working. However it is not the Nambu string. For SU(2) good support for the Nambu string is found for $T_c/\sqrt{\sigma}$. (No sufficiently high statistics data are presently available for the static potential in this case though, so the Nambu string is difficult to verify here.)

Outlook. It is clear that further studies along these lines requires the measurements of nonsuppressed quantities at larger distances. As mentioned in the introduction the inclusion of static charges in the action would accomplish this.

Meanwhile one should use Polyakov loops [16] instead of Wilson loops since the roughening terms are less suppressed in the former. A high statistics Polyakov loop sample for SU(2) would be most welcome.

References

[1] K. Wilson, Phys. Rev. D10 (1974) 2445
[2] M. Creutz, Phys. Rev. D21 (1980) 2308;
E. Brooks III et al., ref. [21]; D. Barkai et al., ref. [22]
[3] Y. Nambu, *in* Symmetries and quark models, ed. R. Chand (Gordon and Breach, New York, 1970)
[4] P. Goddard, J. Goldstone, C. Rebbi and C. Thorn, Nucl. Phys. B56 (1972) 109
[5] H.B. Nielsen and P. Olesen, Nucl. Phys. B61 (1973) 45
[6] M. Lüscher, K. Symanzik and P. Weisz, Nucl. Phys. B173 (1980) 365;
M. Lüscher, Nucl. Phys. B180 [FS2] (1981) 317
[7] M. Fukugita and T. Niuja, Phys. Lett. 132B (1983) 374
[8] J.W. Flower and S.W. Otto, Phys. Lett. 160B (1985) 128
[9] J. Greensite and T. Sterling, Nucl. Phys. B220 [FS8] (1983) 327
[10] L. Sköld and C. Peterson, Nucl. Phys. B255 (1985) 365
[11] J. Ambjørn, M. Flensburg and C. Peterson, Phys. Lett. 159B (1985) 355; Nucl. Phys. B275 [FS17] (1986) 375
[12] O. Alvarez, Phys. Rev. D24 (1981) 440
[13] J.F. Arvis, Phys. Lett. 127B (1983) 106
[14] J. Ambjørn, P. Olesen and C. Peterson, Phys. Lett. 142B (1984) 410; Nucl. Phys. B244 (1984) 262
[15] M. Flensburg and C. Peterson, Phys. Lett. 153B (1985) 412
[16] Ph. de Forcrand, G. Schierholz, H. Schneider and M. Teper, Phys. Lett. 160B (1985) 137
[17] R.D. Pisarski and O. Alvarez, Phys. Rev. D26 (1982) 3735
[18] A. Schild, Phys. Rev. D16 (1977) 1722
[19] K. Dietz and T. Filk, Phys. Rev. D27 (1983) 2944;
T. Filk, Bonn preprint BONN-IR-82-19
[20] Ph. de Forcrand et al., ref. [16]
[21] E. Brooks III et al., Phys. Rev. Lett. 52 (1984) 2324;
S.W. Otto and J.D. Stack, Phys. Rev. Lett 52 (1984) 2328
[22] D. Barkai, K.J.M. Moriarty and C. Rebbi, Phys. Rev. D30 (1984) 1293
[23] E. Kovacs, Phys. Rev. D25 (1982) 871;
J.D. Stack, Phys. Rev. D29 (1984) 1213

[24] R. Sommer and M. Schilling, Wuppertal preprint WU B 85-6
[25] Ph. de Forcrand, 16^4 lattice, compiled by A. Hasenfratz and P. Hasenfratz (CERN, Nov. 1984)
[26] K.C. Bowler, P. Hasenfratz, U. Heller, F. Karsch, R.D. Kenway, I. Montvay, G.S. Pawley, J. Smith and D.J. Wallace, compiled by A. Hasenfratz and P. Hasenfratz (CERN, Nov. 1984)
[27] J.W. Flower and S.W. Otto, private communication
[28] Ph. de Forcrand, 24^4 lattice, compiled by A. Hasenfratz and P. Hasenfratz (CERN, Nov. 1984)
[29] A. Gonzalez-Arroyo and M. Okawa, Phys. Lett. 153B (1983) 415
[30] K. Fabricius and O. Haan, Phys. Lett. 139B (1984) 293
[31] L.D. McLerran and B. Svetitsky, Phys. Lett. 98B (1981) 195; Phys. Rev. D24 (1981) 450
J. Kuti, J. Polonyi and K. Szlachanyi, Phys. Lett. 98B (1981) 199;
J. Engels, F. Karsch, I. Montvay and H. Satz, Phys. Lett. 101B (1981) 89; Nucl. Phys. [FS5] (1982) 545
[32] J. Engels, F. Karsch, H. Satz and I. Montvay, Phys. Lett. 102B (1981) 332; Nucl. Phys. B220 (1983) 223
[33] G. Gurci and R. Tripicioni, Phys. Lett. 151B (1985) 145
[34] J. Engels, J. Jerśak, K. Kanaya, E. Laermann, T. Neuhaus and H. Satz, to be published
[35] J. Kogut et al., Phys. Rev. Lett. 50 (1981) 393;
T. Celik, J. Engels and H. Satz, Phys. Lett. 129B (1983) 323; Z. Phys. C22 (1984) 301;
F. Karsch and R. Petronzio, Phys. Lett. 141B (1984) 105;
B. Svetitsky and F. Fucito, Phys. Lett. 131B (1984) 165;
S.A. Gottlieb et al., Phys. Rev. Lett. 55B (1985) 1958
[36] S.A. Gottlieb, J. Kuti, D. Toussaint, A.D. Kennedy, S. Meyer, B.J. Pendleton and R.D. Sugar, Phys. Rev. Lett. 55 (1985) 1958
[37] N.H. Christ and A.E. Terrano, Phys. Rev. Lett. 56 (1986) 111
[38] F. Fucito, C. Rebbi and S. Solomon, Nucl. Phys. B248 (1984) 615; Phys. Rev. D31 (1985) 1461;
R.G. Gavai, M. Lev and B. Petterson, Phys. Lett. 140B (1984) 397; Phys. Lett. 149B (1984) 492;
J. Polonyi, H.W. Wyld, J.B. Kogut, J. Shigemitsu and D. Sinclair, Phys. Rev. Lett. 53 (1984) 644
[39] K. Fabricius and O. Haan, Nucl. Phys. B260 (1985) 285
[40] S.R. Das and J.B. Kogut, Phys. Rev. D31 (1985) 2704
[41] R.P. Feynman, *in* Proc. 1981 Int. Conf. in High Energy Physics, Lisbon, eds. J. Dias de Deus, J. Soffer
[42] P. Olesen, Phys. Lett. 160B (1985) 408
[43] M. Flensburg and A. Irbäck, Phys. Lett. 175B (1986) 187
[44] F. Karsch and C.B. Lang, Phys. Lett. 138B (1984) 176
[45] J. Ambjørn, P. Olesen and C. Peterson, Nucl. Phys. B240 [FS12] (1984) 189
[46] F. Gutbrod and I. Montvay, Phys. Lett. 136B (1984) 411
[47] A. Billoire and E. Marinari, Phys. Lett. 139B (1984) 399
[48] A. Patel, Nucl. Phys. B243 (1984) 411